



Intrinsic decoherence effects on correlated coherence and quantum discord in XXZ Heisenberg model

Zakaria Dahbi¹ · Mansoura Oumennana² · Mostafa Mansour²

Received: 18 November 2022 / Accepted: 19 January 2023 / Published online: 13 March 2023
© The Author(s), under exclusive licence to Springer Science+Business Media, LLC, part of Springer Nature 2023

Abstract

Spin qubits are at the heart of technological advances in quantum processors and offer an excellent framework for quantum information processing. This work characterizes the time evolution of coherence and nonclassical correlations in a two-spin XXZ Heisenberg model, from which a two-qubit system is realized. We study the effects of intrinsic decoherence on coherence (*correlated coherence*) and nonclassical correlations (*quantum discord*), taking into consideration the combined impact of an external magnetic field, Dzyaloshinsky–Moriya (DM) and Kaplan–Shekhtman–Entin–Wohlman–Aharony (KSEA) interactions. To fully understand the effects of intrinsic decoherence, two extended Werner-like (EWL) states were considered in this work. The findings indicate that intrinsic decoherence leads to a decay in the quantum coherence and quantum correlations and that their behavior depends strongly on the initial EWL state parameters. Likewise, we found that the robustness of correlated coherence and quantum discord can be controlled through an appropriate choice of the initial state. These findings give us insights into engineering a quantum system to achieve quantum advantages.

Keywords Intrinsic decoherence · Spin qubits · Quantum discord · Correlated coherence

1 Introduction

Studying solid-state physical systems under multiple interactions has recently attracted particular focus. The unprecedented possibility of taking advantage of these systems has opened the door to constructing new quantum-based technologies (Dowling and

✉ Zakaria Dahbi
zakaria_dahbi2@um5.ac.ma

Mansoura Oumennana
oum.mans@gmail.com

Mostafa Mansour
mostafa.mansour.fpb@gmail.com

¹ Lab of High Energy Physics-Modeling and Simulation, Faculty of Sciences, Mohammed V University in Rabat, 4 Avenue Ibn Battouta B.P., 1014 RP Rabat, Morocco

² Laboratory of High Energy Physics and Condensed Matter, Department of Physics, Faculty of Sciences Ain Chock, Hassan II University, P.O. Box 5366, Maarif 20100, Casablanca, Morocco

Milburn 2003). Quantum superposition and entanglement (Einstein et al. 1935) are two surprising aspects of the quantum theory and are found to be imperative resources for achieving speedup in information processing (Nielsen and Chuang 2002) and for realizing several non-local tasks and classically unattainable applications (Ekert et al. 1992; Kim et al. 2001; Mansour and Dahbi 2020; Cruz et al. 2022) within the realm of classical physics. Further, it has been demonstrated that even when entanglement is lost, quantum information processing tasks may still be performed in the case of particular mixed states due to the presence of nonclassical correlations beyond entanglement (Adesso et al. 2016; Melo-Luna et al. 2017). On the other side, decoherence (Schlosshauer 2019) effects present a grave challenge to the beneficial applications of quantum mechanics because it prevents the retention and controllable handling of qubits.

Previously many studies focused on measuring and characterizing quantum resources in the framework of intrinsic and standard decoherence models in different quantum systems (Dahbi et al. 2023; Yin et al. 2022; Essakhi et al. 2022; Mohamed and Eleuch 2020; Mohamed et al. 2022; Chaouki et al. 2022; Hashem et al. 2022; Mansour and Dahbi 2020; Haddadi et al. 2022; Maleki 2017; Wu et al. 2017; Li et al. 2021; El Anouz et al. 2022; Mohamed et al. 2022; Mansour et al. 2021; Naveena et al. 2022; Muthuganesan and Chandrasekar 2021). Although many methods were introduced to measure quantum systems, assessing the quantumness of multipartite systems is still a challenging task Adesso et al. (2016); Schlosshauer (2005); Coopmans et al. (2022). For specific quantum systems, quantum discord (QD) Ollivier and Zurek (2001) was the first quantifier introduced to capture nonclassical correlations. QD measures the difference between total correlations and classical correlations in a quantum system. However, it is a strenuous measure to calculate, and analytical expressions of QD were only obtained for two-qubit states (Luo 2008; Henderson and Vedral Aug 2001) and quantum X-states (see for instance the works (Wang et al. 2010; Chen et al. 2011; Haddadi et al. 2019; Baba et al. 2020) and references therein). A rigorous mathematical characterization on the computational difficulties of quantum discord is provided in Huang (2014), demonstrating that computing quantum discord is an NP-complete problem. Quantum correlations have been studied in many quantum systems, such as Heisenberg spin chain models (for instance, spin-1 Heisenberg chains (Malvezzi et al. 2016), anisotropic spin-1/2 XY chain in transverse magnetic field (Mofidnakhaei et al. 2018)) and quantum dot systems such as two coupled double quantum dots systems (Filgueiras et al. 2020; Dahbi et al. 2022; Elghaayda et al. 2022; Ferreira et al. 2022), gravitational cat states (Dahbi et al. 2022), and many other realizable physical systems (Obada et al. 2013; Mohamed and Eleuch 2022; Elghaayda et al. 2022; Mohamed et al. 2022)). Recently, considerable attention has been dedicated to studying the influence of the Dzyaloshinsky-Moriya (DM) interaction and the Kaplan-Shekhtman-Entin-Wohlman-Aharony (KSEA) interaction on the quantum features of specific quantum systems (Oumennana et al. 2022; Khedif et al. 2021; Xie and Liu 2022; Oumennana et al. 2022). The Dzyaloshinsky–Moriya (DM) interaction is a spin-orbit coupling mechanism that induces an antisymmetric exchange that adds to the total magnetic exchange interaction between two nearby spins (more details can be found in Moriya (1960)). The DM Hamiltonian of two spins is found to be $\hat{H}_{DM} = \mathbf{D} \cdot (\mathbf{S}_1 \times \mathbf{S}_2)$, where \mathbf{D} is a constant vector. In addition, Moriya found the second-order correction term, $H_{KSEA} = \mathbf{S}_1 \cdot \Gamma \cdot \mathbf{S}_2$, where Γ is a symmetric traceless tensor. However, he assumed that this term is negligible compared to the antisymmetric contribution until (Kaplan 1983), and then Shekhtman et al. (1992) proved otherwise. It was shown that the symmetric KSEA is important for recovering the broken SU(2) symmetry caused by the DM interaction (Citro and Orignac 2002).

Quantum coherence is another quantum feature that one should deal with. This latter emanates from the superposition principle of quantum states and is a valuable resource to be preserved due to its pivotal role in quantum information processing (Pan et al. 2017) and quantum thermodynamics (Narasimhachar and Gour 2015). It was indeed proven that long-lasting quantum coherence is vital for overcoming classical limitations of measurement accuracy in quantum metrology (Pires et al. 2018). Moreover, growing interest is accorded to the role played by quantum coherence in some biological mechanisms (Lambert et al. 2013), such as photosynthesis (Scholes 2011) and bird navigation (Ritz 2011). Similarly to quantum correlations and entanglement, several quantifiers were introduced to capture quantum coherence in quantum systems appropriately, *e.g.* relative entropy of coherence and l_1 -norm of coherence (Baumgratz et al. 2014) as well as intrinsic randomness (Yuan et al. 2015).

In this article, we investigate the evolution of correlated coherence and quantum correlations quantified by quantum discord in a two-qubit XXZ Heisenberg spin chain under intrinsic decoherence effects with an applied magnetic field, KSEA and DM interactions using the Milburn's decoherence model (Milburn 1991). We mainly focus on how the Hamiltonian parameters and the initial state affect the dynamical behavior of correlated coherence and quantum discord. We look at two different extended Werner-like states to show how the choice of the initial state is essential to suppress the effects of specific interactions.

The rest of this work is as follows. In Sect. 2, we give a short overview of the quantum resources indicators used in this study. The Hamiltonian of the considered physical model is introduced in Sect. 3, and the evolved density matrix corresponding to the system is derived for the parameterized initial state considered. In Sect. 4 we present the results obtained for the dynamics of correlated coherence and quantum discord under the influence of intrinsic decoherence with the combined impact of KSEA and DM interactions. Finally, we conclude the main findings from the proposed model in Sect. 5.

2 Quantum information indicators

This part defines the correlated coherence, used as a quantum coherence quantifier, and the quantum discord operated to quantify nonclassical correlations.

2.1 Correlated coherence

Quantum coherence is a basis-dependent property of a quantum state that arises from the superposition of system states reflected by the non-diagonal components of the density matrix on a given basis. Here, we consider a conveniently computable coherence measure, specifically the l_1 -norm of coherence (Baumgratz et al. 2014). The l_1 -norm of coherence is a trustworthy key indicator that meets the requirements of a good coherence measure and can be obtained for a given density matrix ρ . Baumgratz *et al.* (Baumgratz et al. 2014) has demonstrated that a quantum system's coherence is given as

$$C_{l_1}(\rho) = \min_{\eta \in \mathfrak{I}} |\rho - \eta|, \quad (1)$$

where \mathfrak{I} is a set containing all incoherent states, that is $C_{l_1}(\eta) = 0$ for all $\eta \in \mathfrak{I}$. The l_1 -norm coherence can be obtained by means of the non-diagonal entries of ρ as

$$C_{l_1}(\rho) = \sum_{i \neq j} \sqrt{\rho_{ij} \rho_{ij}^*}, \tag{2}$$

where ρ_{ij}^* refers to the complex conjugate. It should be noted that the total l_1 -norm coherence of a state ρ , living in Hilbert space of dimension d , should not exceed $d - 1$. Correlated coherence is yet another metric of coherence that can provide information about the quantumness of a particular state. For any given bipartite state ρ , correlated coherence is defined as the total coherence subtracting local coherences. The definition of the l_1 -norm based correlated coherence (Baumgratz et al. 2014) reads as

$$C_{cc}(\rho) := C_{l_1}(\rho) - C_{l_1}(\rho_A) - C_{l_1}(\rho_B), \tag{3}$$

where $\rho_A = \text{tr}_B \rho$ and $\rho_B = \text{tr}_A \rho$ are the reduced density matrices of local subsystems.

2.2 Quantum discord

QD (Ollivier and Zurek 2001) quantifies quantum correlations inhibited in a composite system. In a two-qubit system, QD is defined by removing the existing classical correlations from the quantum mutual information of the system as

$$\mathcal{D}(\rho) = \mathcal{I}(\rho) - \mathcal{C}(\rho), \tag{4}$$

with

$$\mathcal{I}(\rho) = \mathcal{S}(\rho_B) + \mathcal{S}(\rho_A) - \mathcal{S}(\rho) \tag{5}$$

and

$$\mathcal{C}(\rho) = \mathcal{S}(\rho_A) - \min_{\{\pi_B^i\}} \sum_i p_i \mathcal{S}(\rho_{A|i}). \tag{6}$$

$\mathcal{S}(\rho) = -\text{tr}(\rho \log_2 \rho)$ is the von Neumann entropy. ρ_A and ρ_B are the reduced density operators corresponding, respectively, to the subsystems A and B . $\{\pi_B^i\} = |i_B\rangle\langle i_B|$ is the complete ensemble of orthonormal projectors acting only on the second subsystem B .

$\rho_{A|i} = \text{tr}_B(\pi_B^i \rho \pi_B^i) / p_i$ is the resulting state of the first subsystem A after obtaining the result i on B , and $p_i = \text{tr}_{AB}(\pi_B^i \rho \pi_B^i)$ is the probability of having i as a result. Following the relations (5) and (6), the quantum discord (4) can be rewritten as Henderson and Vedral (2001); Fanchini et al. (2010)

$$\mathcal{D}(\rho) = \min_{\{\pi_B^i\}} [\mathcal{S}(\rho / \{\pi_B^i\})] + \mathcal{S}(\rho_B) - \mathcal{S}(\rho). \tag{7}$$

In general, for arbitrary quantum states, finding analytical formulas for QD is complicated due to the minimization process required for conditional entropy. It was only possible to obtain approximate analytical expressions (Huang 2013) for a limited number of states, such as the X -states. For X -states

$$\rho = \begin{bmatrix} \rho_{11} & 0 & 0 & \rho_{14}^* \\ 0 & \rho_{22} & \rho_{23}^* & 0 \\ 0 & \rho_{23} & \rho_{33} & 0 \\ \rho_{14} & 0 & 0 & \rho_{44} \end{bmatrix} \tag{8}$$

the quantum discord is redefined by the succeeding expression (Wang et al. 2010; Ali et al. 2010)

$$\mathcal{D}(\rho) = \min\{\mathcal{QD}_1, \mathcal{QD}_2\}, \tag{9}$$

with

$$\mathcal{QD}_i = f(\rho_{11} + \rho_{33}) + \sum_{k=1}^4 \lambda_k \log_2(\lambda_k) + \mathcal{D}_i.$$

$\mathcal{D}_1 = f(\Lambda), \mathcal{D}_2 = -\sum_{m=1}^4 \rho_{mm} \log_2(\rho_{mm}) - f(\rho_{11} + \rho_{33}), \Lambda = \frac{1}{2} \left(1 + \left((1 - 2(\rho_{33} + \rho_{44}))^2 + 4(|\rho_{14}| + |\rho_{23}|)^2 \right)^{1/2} \right)$ and $f(x) = -x \log_2(x) - (1 - x) \log_2(1 - x)$ is the binary Shannon entropy. λ_k 's denote the eigenvalues of the density matrix ρ .

As a point worth highlighting here, it was demonstrated in Ref. (Tan et al. 2016) that correlated coherence can unify numerous ideas of quantumness, such as quantum discord, within the same paradigm and that the concept of correlated coherence recognizes similarities between quantum correlations and quantum entanglement. So, the quantum features of correlations derive from the quantum features of coherence.

3 Two-qubit XXZ model

We consider the model as a two-qubit system operating spin polarization of two nearest spin-1/2 XXZ particles. The particles are exposed to the interplay of an external homogeneous magnetic field and the combination of DM and KSEA interactions along the z -axis. The associated Hamiltonian is solvable and is represented as Oumennana et al. (2022)

$$\begin{aligned} \hat{H} = & J_z \sigma_1^z \sigma_2^z + J(\sigma_1^x \sigma_2^x + \sigma_1^y \sigma_2^y) + D_z (\sigma_1^x \sigma_2^y - \sigma_1^y \sigma_2^x) \\ & + \Gamma_z (\sigma_1^x \sigma_2^y + \sigma_1^y \sigma_2^x) + B(\sigma_1^z + \sigma_2^z), \end{aligned} \tag{10}$$

where $\sigma_\mu^{i=x,y,z}$ ($\mu = 1, 2$) are the typical Pauli matrices corresponding to the spin μ , while J_z and J are real coupling coefficients denoting, respectively, the anisotropy coupling constant defining the symmetric spin-spin exchange interaction in the z -direction, and the interaction coupling constant. The B is a parameter, restricted to $B \geq 0$, that indicates the strength of the magnetic field. Besides, the Γ_z and D_z parameters reflect the z -KSEA and z -DM interactions, which result in symmetric and anti-symmetric spin-orbit coupling contributions, respectively. We assume that the two-spin XXZ model behaves as in the antiferromagnetic case, $J > 0$ and $J_z > 0$. It is worth stating that all parameters are considered to be dimensionless. The Hamiltonian (10) can be written on the two-qubit basis, $\{|\downarrow\downarrow\rangle, |\downarrow\uparrow\rangle, |\uparrow\downarrow\rangle, |\uparrow\uparrow\rangle\}$, as

$$\hat{H} = \begin{pmatrix} J_z + 2B & 0 & 0 & -2i\Gamma_z \\ 0 & -J_z & 2J + 2iD_z & 0 \\ 0 & -2iD_z + 2J & -J_z & 0 \\ 2i\Gamma_z & 0 & 0 & -2B + J_z \end{pmatrix}. \tag{11}$$

The eigenvalues and the associated eigenvectors of the aforementioned Hamiltonian \hat{H} are

$$\begin{aligned} \mathcal{V}_1 &= J_z + \chi, & \mathcal{V}_2 &= -J_z + \omega, \\ \mathcal{V}_3 &= -J_z - \omega, & \mathcal{V}_4 &= J_z - \chi, \end{aligned}$$

$$\begin{aligned} |u_1\rangle &= \sqrt{\frac{\chi + 2B}{2\chi}} \left(|\Downarrow\Downarrow\rangle + \frac{2i\Gamma_z}{\chi + 2B} |\Uparrow\Uparrow\rangle \right), \\ |u_2\rangle &= \frac{1}{\sqrt{2}} \left(|\Downarrow\Uparrow\rangle + \frac{2J - 2iD_z}{\omega} |\Uparrow\Downarrow\rangle \right), \\ |u_3\rangle &= \frac{1}{\sqrt{2}} \left(|\Downarrow\Uparrow\rangle - \frac{2J - 2iD_z}{\omega} |\Uparrow\Downarrow\rangle \right), \\ |u_4\rangle &= \sqrt{\frac{\chi - 2B}{2\chi}} \left(|\Downarrow\Downarrow\rangle - \frac{2i\Gamma_z}{\chi - 2B} |\Uparrow\Uparrow\rangle \right), \end{aligned}$$

with $\chi = 2(B^2 + \Gamma_z^2)^{1/2}$ and $\omega = 2(J^2 + D_z^2)^{1/2}$. To introduce intrinsic decoherence, we use Milburn’s decoherence model (Milburn 1991), which assumes that quantum systems evolve continually in an arbitrary sequence of identical unitary transformations instead of unitary evolution. The following equation describes such evolution (Milburn 1991)

$$\frac{d\rho_t}{dt} = \frac{1}{\gamma} \left(\exp(-i\gamma\hat{H})\rho_t \exp(i\gamma\hat{H}) - \rho_t \right), \tag{12}$$

here, ρ_t is the density matrix associated to the Hamiltonian \hat{H} , and γ is the intrinsic decoherence parameter. Thus in the limit of $\gamma^{-1} \rightarrow \infty$, there is no intrinsic decoherence, and Eq. (12) is reduced to the typical von Neumann equation characterizing an isolated quantum system. Milburn altered the Schrödinger equation in order for quantum coherence to be spontaneously destroyed throughout the evolution of the quantum system. The ensuing equation is obtained

$$\frac{d\rho_t}{dt} = -\frac{\gamma}{2} [\hat{H}, [\hat{H}, \rho_t]] - i[\hat{H}, \rho_t]. \tag{13}$$

where $\frac{\gamma}{2} [\hat{H}, [\hat{H}, \rho_t]]$ designates the non-unitary evolution under the intrinsic decoherence in our considered two-qubit system. A proper solution for the equation (13) is obtained using the Kraus operators \hat{M}_l (Milburn 1991)

$$\rho_t = \sum_{l=0}^{\infty} \hat{M}_l(t) \rho^{t=0} \hat{M}_l^\dagger(t) \tag{14}$$

with $\rho^{t=0}$ being the density matrix at $t = 0$ of the considered system and \hat{M}_l are given by

$$\hat{M}_l(t) = \left(\frac{\gamma^l t^l}{l!} \right)^{1/2} \hat{H}^l \exp(-i\hat{H}t) \exp\left(-\frac{\gamma t}{2} \hat{H}^2\right),$$

with $\sum_{l=0}^{\infty} \hat{M}_l(t) \hat{M}_l^\dagger(t) = \mathbb{1}$. Finally, the evolved state of the two-spin XXZ quantum system described by \hat{H} under intrinsic decoherence effects can be obtained by Milburn (1991)

$$\rho_t = \sum_{j,k} \exp\left(-\frac{\gamma t}{2}(\mathcal{V}_j - \mathcal{V}_k)^2 - i(\mathcal{V}_j - \mathcal{V}_k)t\right) \times \langle u_j | \rho^{t=0} | u_k \rangle | u_j \rangle \langle u_k |, \tag{15}$$

where $\mathcal{V}_{j,k}$ and $|u_{j,k}\rangle$ are, respectively, the eigenvalues of the Hamiltonian \hat{H} (11) and their corresponding eigenstates. The time-dependent density matrix in Eq. (15) represents the state of the two-qubit XXZ Heisenberg spin model at some time t . It is written as a function of an initial state $\rho^{t=0}$, which will be considered in the following to be a Werner-like state. Equation (15) allows us to describe how the system resources change as the state of the system is evolving under the intrinsic decoherence effects characterized by γ . Following, we use correlated coherence and quantum discord to study how intrinsic decoherence affects coherence and nonclassical correlations in the two-spin XXZ Heisenberg model under the different supposed interactions. For a complete characterization of the influence of intrinsic decoherence on the system, we take into account two possible scenarios of the initial state

$$|\Psi_1\rangle = \cos(\theta/2) |\downarrow\downarrow\rangle + \sin(\theta/2) |\uparrow\uparrow\rangle, \tag{16}$$

$$|\Psi_2\rangle = \cos(\theta/2) |\downarrow\uparrow\rangle + \sin(\theta/2) |\uparrow\downarrow\rangle. \tag{17}$$

where $|0\rangle \equiv |\downarrow\rangle$ and $|1\rangle \equiv |\uparrow\rangle$, denoting spin-down and spin-up, respectively. We shall study intrinsic decoherence according to two samples of Bell-like initial states. To do that, we combine the states in Eqs. (16)–(17) using a parametrization and then solve the dynamical equation. The results for each sample initial state can be obtained by dealing with the parametrization parameters. Thus, the initial state looks as follows

$$\rho^{t=0} = \alpha_1 \rho_1^{t=0} + \alpha_2 \rho_2^{t=0}, \tag{18}$$

where $\rho_i^{t=0} = p |\Psi_i\rangle \langle \Psi_i| + (1-p)/4 I_4$, $0 \leq p \leq 1$ denoting the level of purity in the initial state, $0 \leq \theta < \pi$ and α_1 and α_2 are the parametrization parameters taking either zero or one in each of the two scenarios. We note that when Bell-like states reduce to Bell states, those of EWL states reduce to Werner states (Werner 1989). The parameterized initial state is follows

$$\rho^{t=0} = \begin{pmatrix} \frac{1}{4} (\alpha_1 (2p \cos(\theta) + p + 1) - \alpha_2 (p - 1)) & 0 & 0 & \frac{1}{2} \alpha_1 p \sin(\theta) \\ 0 & \frac{1}{4} (\alpha_2 (2p \cos(\theta) + p + 1) - \alpha_1 (p - 1)) & \frac{1}{2} \alpha_2 p \sin(\theta) & 0 \\ 0 & \frac{1}{2} \alpha_2 p \sin(\theta) & \frac{1}{4} (\alpha_2 (-2p \cos(\theta) + p + 1) - \alpha_1 (p - 1)) & 0 \\ \frac{1}{2} \alpha_1 p \sin(\theta) & 0 & 0 & \frac{1}{4} (\alpha_1 (-2p \cos(\theta) + p + 1) - \alpha_2 (p - 1)) \end{pmatrix}.$$

To simplify calculations, all terms that correspond to the product $\alpha_1 \alpha_2$ in ρ^t cancel in both situations and thus can be omitted. By solving the Milburn’s equation, one finds that the time-dependent density matrix encoding both cases takes the form

$$\rho^t = \begin{pmatrix} \rho_{11} & 0 & 0 & \rho_{14} \\ 0 & \rho_{22} & \rho_{23} & 0 \\ 0 & \rho_{23}^* & \rho_{33} & 0 \\ \rho_{14}^* & 0 & 0 & \rho_{44} \end{pmatrix}. \tag{19}$$

The time-evolution preserves the X-structure of the initial extended Werner-like (EWL) state for any choice between the two initial states. The following table gives the properties of the density matrix for each case.

$ \Psi_i\rangle$	(α_1, α_2)	$\varrho_{ij} \neq 0$
$ \Psi_1\rangle$	$(1, 0)$	$(\varrho_{11}, \varrho_{14}, \varrho_{22}, \varrho_{44})$, with $\varrho_{33} = \varrho_{22}, \varrho_{41} = \varrho_{14}^*$
$ \Psi_2\rangle$	$(0, 1)$	$(\varrho_{11}, \varrho_{22}, \varrho_{23}, \varrho_{33})$, with $\varrho_{11} = \varrho_{44}, \varrho_{32} = \varrho_{23}^*$

For the combined initial state in (18), we get the following density matrix entries

$$\begin{aligned} \varrho_{11} &= \frac{\alpha_1}{\chi^2} \left(B^2(2p \cos(\theta) + p + 1) + p\Gamma_z e^{-2\gamma t \chi^2} (2 \cos(\theta)\Gamma_z \cos(2t\chi) - \chi \sin(\theta) \sin(2t\chi)) + (p + 1)\Gamma_z^2 \right) - \frac{1}{4}\alpha_2(p - 1), \\ \varrho_{14} &= \frac{\alpha_1 p e^{-2\gamma t \chi^2}}{2\chi^2} \left(\chi \sin(\theta)(\chi \cos(2t\chi) - 2iB \sin(2t\chi)) + 2 \cos(\theta)\Gamma_z (-2iB e^{2\gamma t \chi^2} + 2iB \cos(2t\chi) + \chi \sin(2t\chi)) \right), \\ \varrho_{22} &= \frac{\alpha_2}{4\omega} \left((2p e^{-2\gamma t \omega^2} ((2D_z \sin(\theta) \sin(2t\omega) + \omega \cos(\theta) \cos(2t\omega)) + (p + 1)\omega) - \alpha_1(p - 1)\omega) \right), \\ \varrho_{23} &= \frac{\alpha_2 p e^{-2\gamma t \omega^2}}{\omega^2} (J - iD_z) (-2iD_z \sin(\theta) \cos(2t\omega) + 2J \sin(\theta) e^{2\gamma t \omega^2} + i\omega \cos(\theta) \sin(2t\omega)), \\ \varrho_{33} &= \frac{\alpha_2}{4\omega} \left((p + 1)\omega - 2p e^{-2\gamma t \omega^2} (2D_z \sin(\theta) \sin(2t\omega) + \omega \cos(\theta) \cos(2t\omega)) \right) - \alpha_1(p - 1)\omega, \\ \varrho_{44} &= \frac{\alpha_1}{\chi^2} \left(B^2(-2p \cos(\theta) + p + 1) + p\Gamma_z e^{-2\gamma t \chi^2} (\chi \sin(\theta) \sin(2t\chi) - 2 \cos(\theta)\Gamma_z \cos(2t\chi)) + (p + 1)\Gamma_z^2 \right) - \frac{1}{4}\alpha_2(p - 1). \end{aligned}$$

The populations of the system combining both scenarios are given implicitly as

$$\begin{aligned} \lambda_1 &= \frac{1}{2} \left(-\sqrt{4|\varrho_{23}|^2 + (\varrho_{22} - \varrho_{33})^2} + \varrho_{22} + \varrho_{33} \right), \\ \lambda_2 &= \frac{1}{2} \left(\sqrt{4|\varrho_{23}|^2 + (\varrho_{22} - \varrho_{33})^2} + \varrho_{22} + \varrho_{33} \right), \\ \lambda_3 &= \frac{1}{2} \left(-\sqrt{4|\varrho_{14}|^2 + (\varrho_{11} - \varrho_{44})^2} + \varrho_{11} + \varrho_{44} \right), \\ \lambda_4 &= \frac{1}{2} \left(\sqrt{4|\varrho_{14}|^2 + (\varrho_{11} - \varrho_{44})^2} + \varrho_{11} + \varrho_{44} \right). \end{aligned}$$

We use the following notation to locate the matrix density and populations for each case:

$$\varrho^f = \begin{cases} \varrho_1^f, & \text{if } \alpha_1 = 1, \alpha_2 = 0 \\ \varrho_2^f, & \text{if } \alpha_1 = 0, \alpha_2 = 1 \end{cases} \tag{20}$$

By combining the two cases in (20), correlated coherence writes as

$$\begin{aligned}
 C_{cc}(\rho^t) = & \frac{\alpha_1 p e^{-2\gamma t \chi^2}}{\chi^2} \left[\left(2B\chi \sin(\theta) \sin(2t\chi) + 4B \cos(\theta) \right. \right. \\
 & \times \Gamma_z \left(e^{2\gamma t \chi^2} - \cos(2t\chi) \right) \left. \left. \right)^2 \right. \\
 & \left. + \left(\chi^2 \sin(\theta) \cos(2t\chi) + 2\chi \cos(\theta) \Gamma_z \sin(2t\chi) \right)^2 \right]^{1/2} \tag{21} \\
 & + \frac{\alpha_2 p e^{-2\gamma t \omega^2}}{\omega} \left[\left(\omega \cos(\theta) \sin(2t\omega) - 2D_z \sin(\theta) \right. \right. \\
 & \times \cos(2t\omega) \left. \left. \right)^2 + 4J^2 \sin^2(\theta) e^{4\gamma t \omega^2} \right]^{1/2}.
 \end{aligned}$$

One can check that ρ_{14} and ρ_{23} are the sole non-zero off-diagonal elements, storing all information about the system’s coherence for each studied case. As well, one can easily verify that local coherence, ($C^L(\rho) = C_{l_1}(\rho_A) + C_{l_1}(\rho_B) = 0$), is always zero and thus correlated coherence is the system’s total coherence. Similarly, quantum discord is obtained implicitly as

$$\begin{aligned}
 QD_1 = & \log_2 \left(\frac{(1 - \Lambda)^\Lambda}{\Lambda^\Lambda - \Lambda^{\Lambda+1}} \prod_{i=1}^4 \lambda_i^{\lambda_i} \left(\frac{\beta}{1 - \beta} \right)^{-\beta} \right) \\
 & - \log_2(-\beta + 1), \tag{22}
 \end{aligned}$$

$$QD_2 = \log_2 \left(\prod_{i=1}^4 \lambda_i^{\lambda_i} \times \prod_{j=1}^4 \rho_{jj}^{-\rho_{jj}} \right), \tag{23}$$

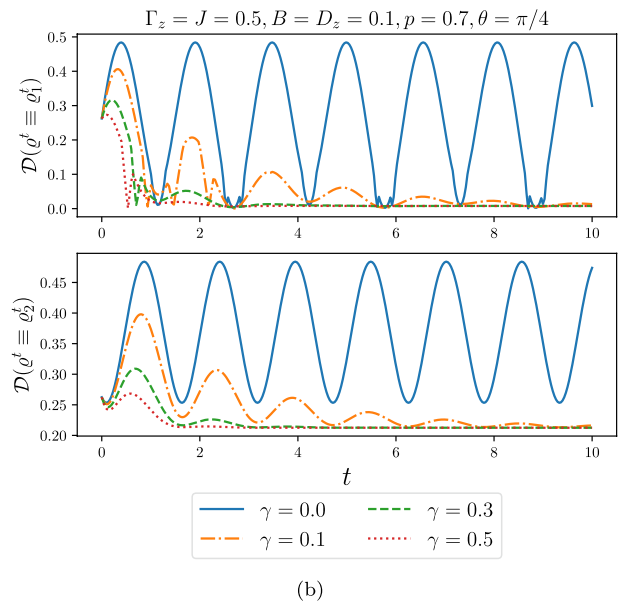
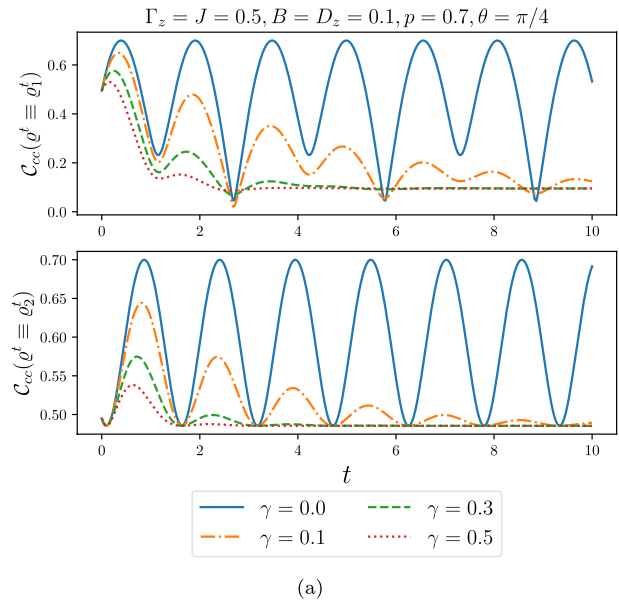
where $\Lambda = \frac{1}{2} \left(\sqrt{4(\rho_{14} + \rho_{23})^2 + (1 - 2(\rho_{33} + \rho_{44}))^2} + 1 \right)$, $\beta = \rho_{11} + \rho_{33}$ and λ_i ’s are the populations of the system. Quantum discord is then computed by plugging Eq. (22) and Eq. (23) in Eq. (9).

4 Results and analysis

This section presents the obtained findings regarding correlated coherence and quantum discord. To sweeten our learning of the dynamical aspect of quantum correlations and coherence in the two-qubit XXZ Heisenberg model, we considered two kinds of EWL states. We then depict the behavior of coherence and quantum correlations as a function of time and all the parameters in the Hamiltonian as well as the level of purity of the initial state, the Bloch angle, and the decoherence rate.

In Fig. 1, we plot the correlated coherence and quantum discord as functions of time t for both initial EWL states $\rho_1^{t=0}$ and $\rho_2^{t=0}$ for some decoherence rates γ . We notice that both measures show oscillatory behavior due to intrinsic decoherence. At the initial time $t = 0$, the two quantifiers start from the same equal nonzero value for both initial states $\rho_1^{t=0}$ and $\rho_2^{t=0}$, that is $C_{cc}(\rho_1^{t=0}) = C_{cc}(\rho_2^{t=0}) \approx 0.495$ and $\mathcal{D}(\rho_1^{t=0}) = \mathcal{D}(\rho_2^{t=0}) \approx 0.262$. Without intrinsic decoherence $\gamma = 0$, both measures display non-damping oscillations and fluctuate between their minimum and maximum values for an infinite time scale. For $\gamma > 0$, as time increases,

Fig. 1 Time-evolution of coherence (correlated coherence) **a** and quantum correlations (quantum discord) **b**. Case 1 ($\rho^t \equiv \rho_1^t$) and case 2 ($\rho^t \equiv \rho_2^t$), versus decoherence rates γ



correlated coherence and quantum discord experience damped oscillations and get closer to a stable value after an adequate period suggesting that the system has evolved to a steady state. When $t \rightarrow +\infty$, the attained steady state becomes independent on γ but on the initial Werner-like state and the Hamiltonian parameters, namely p and θ . Also, it is marked that a more considerable γ drives the quick decline of correlated coherence and discord; it causes the number and size of their oscillations to drop at some point, causing the system's state to transition into a steady state quickly. The coherence and correlation deterioration are due to

the damping terms $e^{-2\gamma t \chi^2}$ (in the case of ρ_1^t) and $e^{-2\gamma t \omega^2}$ (in the case of ρ_2^t); these functions reduce the coherence and quantum correlations amplitude after each incrementing t or γ . Similarly, we can mark identical routines for all the different cases.

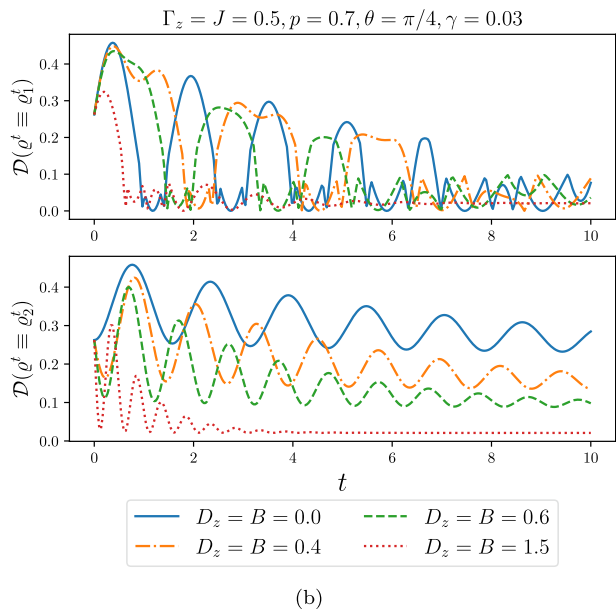
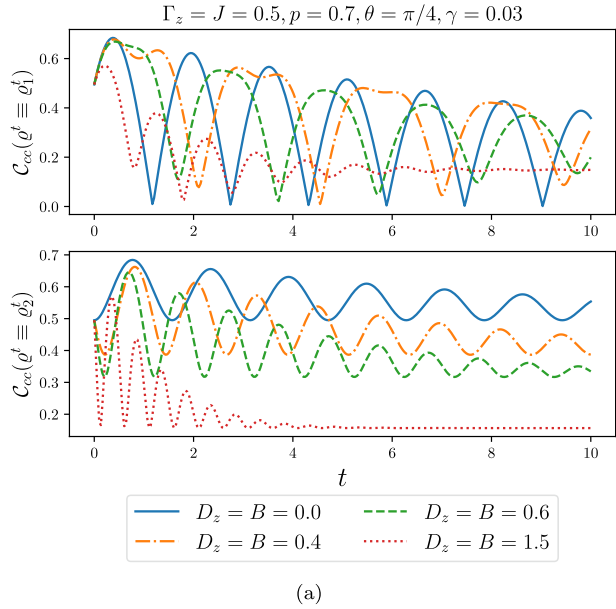
In the asymptotic limit, $t \rightarrow \infty$, quantum coherence and quantum correlations reach their stable value. The higher the steady-state correlation, the more the system will be appropriate for achieving quantum-based tasks. In the same conditions of $\Gamma_z = J = 0.5, B = D_z = 0.1, p = 0.7, \theta = \pi/4$ and $\gamma > 0$, we numerically find the value of correlated coherence as $C_{cc}(\rho_1^{t \rightarrow \infty}) \approx 0.095$ and $C_{cc}(\rho_2^{t \rightarrow \infty}) \approx 0.485$. Similarly, for quantum discord, we find $\mathcal{D}(\rho_1^{t \rightarrow \infty}) \approx 0.007$ and $\mathcal{D}(\rho_2^{t \rightarrow \infty}) \approx 0.212$.

Remarkably, we encountered that $C_{cc}(\rho_1^{t \rightarrow \infty}) < C_{cc}(\rho_2^{t \rightarrow \infty})$ and $\mathcal{D}(\rho_1^{t \rightarrow \infty}) < \mathcal{D}(\rho_2^{t \rightarrow \infty})$, this means that the system sustains more superposition and correlations when it is prepared in the initial state $\rho_2^{t=0}$. On the other hand, when the system is initially prepared in the Werner-like state $\rho_1^{t=0}$, its steady state is still a weakly correlated mixed state that sustains low superposition.

Figure 2 shows the dynamics of correlated coherence and quantum discord versus time t for various values of the DM interaction strength D_z and the homogeneous magnetic field B . It is worth noting, as it was shown analytically above, that the DM interaction does not affect the system when the considered initial state is $\rho_1^{t=0}$ as D_z does not appear in the expressions of the entries of the evolved density matrix ρ_1^t . Likewise, the effect of the magnetic field B can not be studied for ρ_2^t since the structure of the initial EWL state $\rho_2^{t=0}$ totally suppresses its contribution.

In Fig. 2a, we notice that for growing intensities of the magnetic field B , the oscillatory behavior of correlated coherence within ρ_1^t swiftly declines as the amplitudes are shrinking, and $C_{cc}(\rho_1^t)$ rapidly stabilizes on a nonzero frozen state. Furthermore, the oscillations are slightly phase-shifted, and when $B \neq 0$, the peaks presenting the maximal values reached over time are broader for more diminutive intensities of B . We again observe that the lower bound of the oscillations is unsteady, as it can increase or decrease over time. When the external magnetic field is non-existing ($B = 0$), correlations are damped over time due to intrinsic decoherence, and we regard the collapse and regeneration phenomena. On the other hand, quantum discord (Fig. 2b) exhibits erratic oscillations; they are indeed damped over time but present successive small and irregular spikes. Physically, since the Milburn model is characterized by the associated magnetic field B , the irregular oscillatory behavior of correlated coherence and discord in the case $\rho^t \equiv \rho_1^t$, could be due to an ongoing information flow between the magnetic field and the two-qubit XXZ spin system. For the second density matrix $\rho^t \equiv \rho_2^t$, we see that the same behavior is manifested by both quantum measures with the mere difference that oscillations are regular and that correlated coherence records higher values than quantum discord. At $t = 0$, the quantum correlations and correlated coherence amounts are nonzero. Their initial recorded quantities do not depend on the DM interaction's strength D_z since they are fixed when the initial state is given. In the absence of the DM interaction $D_z = 0$, both measures record the highest values. In contrast, for increasing D_z values, the oscillations' frequency increases despite being quickly damped. The oscillations get damped and saturate to a stable value for a finite time. This might be explained through the many-body localization-delocalization viewpoint (Doggen et al. 2018). Meanwhile, for $\rho^t \equiv \rho_1^t$ and $\gamma > 0$, the steady states of correlated coherence and discord are closely related to both B and Γ_z , it turns out that there is a competition between B and Γ_z . In more specific terms, the steady states increase/decrease by increasing/decreasing either B or Γ_z until $B = \Gamma_z$, the point at which the steady-state reaches its maximum value. This result indicates that B and Γ_z cancel each other so that the steady states

Fig. 2 Time-evolution of coherence (correlated coherence) **a** and quantum correlations (quantum discord) **b**. Case 1 ($\rho^t \equiv \rho_1^t$): versus B . Case 2 ($\rho^t \equiv \rho_2^t$): versus D_z



of correlated coherence and discord remain dependent only on p and θ . We note that for all $\gamma > 0$, the maximum steady state recorded for $\theta = \pi/4$ and $p = 0.7$ remains constant for all nonzero intensities $B = \Gamma_z$, numerically, $C_{cc}(\rho_1^{t \rightarrow \infty}) \approx 0.2474$ and $\mathcal{D}(\rho_1^{t \rightarrow \infty}) \approx 0.0543$.

For the second configuration $\rho^t \equiv \rho_2^t$, we see that as the DM interaction strength grows, the value of the steady state decreases. In contrast, the steady state of correlated coherence and quantum discord improves as the spin-spin interaction coupling becomes strong.

For $\gamma > 0$ and $J = D_z \neq 0$, the steady state can be modified by changing p and θ . These results highlight the initial state's impact on the system's whole evolution and suggest that its quantum resources could be tweaked and enhanced by modifying certain parameters.

In Fig. 3, we depict the influence of the strength of the KSEA interaction (Γ_z) and the spin-spin coupling J on correlated coherence and quantum discord for both considered initial states. We specify again that the effect of the first parameter is examined only in the first case where $\rho^t \equiv \rho_1^t$, while the influence of the anisotropy parameter J can solely be examined when $\rho^t \equiv \rho_2^t$.

The first salient observation regarding the evolution of correlated coherence and quantum discord in the first considered case $\rho^t \equiv \rho_1^t$, is that both appear to be stable for $\Gamma_z = 0$ for short periods. However, they eventually decrease for sufficiently long periods. In the absence of the KSEA interaction, the expression of correlated coherence reduces to $C_{cc}(\rho_1^t) = pe^{-2\gamma t \times 4B^2} \sin \theta$, and we can numerically perceive its time evolution. Correlated coherence exhibits the same oscillatory pattern in the presence of the KSEA interaction ($\Gamma_z \neq 0$). However, as Γ_z decreases, the lower bound of oscillations is higher, and the minimum values shift to the right. As KSEA interaction strengthens, the frequency of oscillations decreases and coherence becomes less erratic. Quantum discord displays identical behavior as correlated coherence with lower quantities. In distinction, we spot in the dynamical behavior of QD the resurgence of the collapse and revival phenomena and the previously mentioned pattern of minor successive increases and decreases when oscillations reach their minimum values.

In the second case $\rho^t \equiv \rho_2^t$, we observe that for increasing interaction coupling constant J , the frequency of oscillations of both quantifiers increases, but the amplitudes shrink. For $J = 0$, the lower bounds of both measures nearly drop to zero at the same instants t , at $t \approx 2$ and $t \approx 10$, and we see that correlated coherence displays sharp peaks at these instants. Once again, it is apparent that the initial amounts of quantum correlations and correlated coherence are not related to the parameters that do not figure in the initial state.

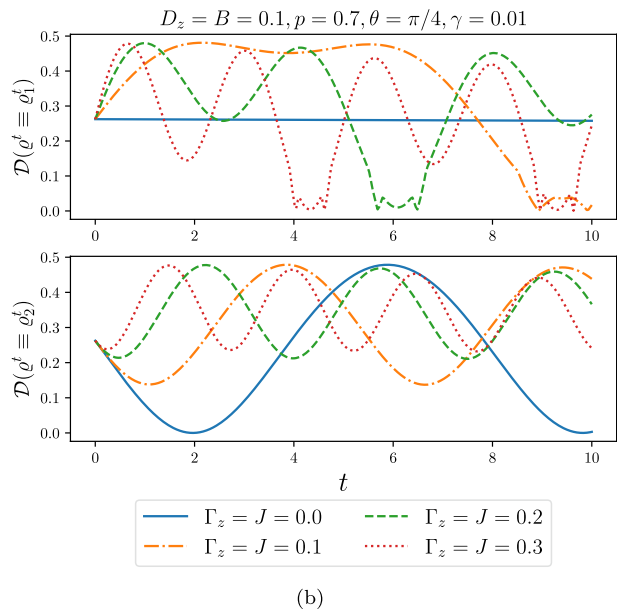
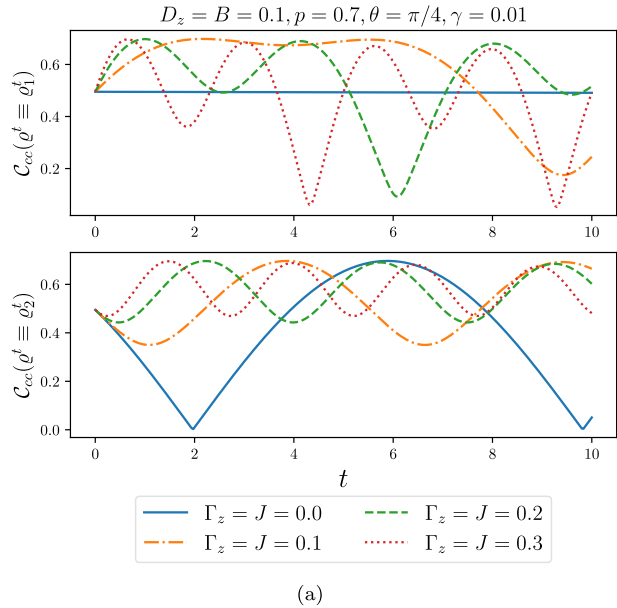
In Fig. 4, we visualize the effect of the angle θ on correlated coherence and quantum discord dynamics. Unlike the previous figures where the initial values, at $t = 0$, of $C_{cc}(\rho^t)$ and $\mathcal{D}(\rho^t)$ are not dependent on the strengths of the parameters γ (Fig. 1), D_z and B (Fig. 2), J and Γ_z (Fig. 3), we notice in Fig. 4 that the initial amounts of quantum correlations and correlated coherence are related to the value of the angle θ .

Clearly, as the value of θ rises, not only the initial recorded values are higher, but also those recorded during the time evolution. The angle θ does not affect the frequency of oscillations, but it affects the quantities of correlated coherence and nonclassical correlations within the system. Moreover, oscillations are in phase when $\rho^t \equiv \rho_2^t$, unlike the first case $\rho^t \equiv \rho_1^t$ where oscillations are slightly phase-shifted to the right for decreasing θ values.

For $\theta = \frac{\pi}{2}$, which is the angle value for which the Bell-like states (16–17) reduce to the maximally entangled Bell states and the EWL becomes a Werner state, $C_{cc}(\rho^t)$ and $\mathcal{D}(\rho^t)$, present the higher quantities. Still, they are roughly invariant as they present timid fluctuations when $\rho^t \equiv \rho_2^t$. Another worth noting remark is the collapse and revival phenomena exhibited in the dynamical behavior of quantum discord when $\rho^t \equiv \rho_1^t$, in addition to the pattern of the small spikes in the lower bound of QD.

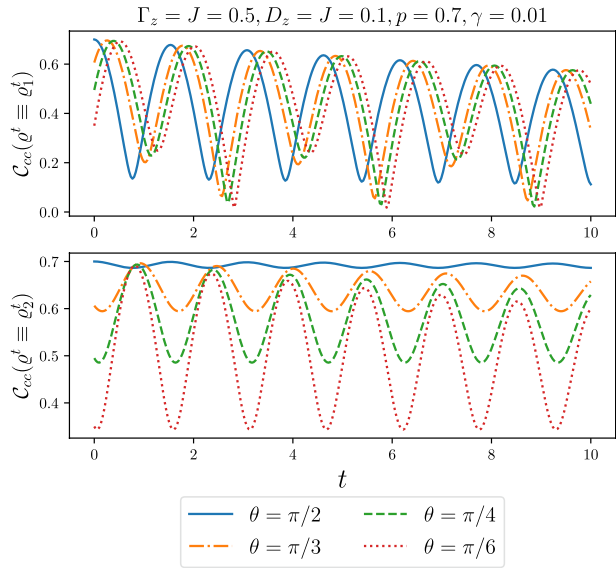
In Fig. 5, we show the impact of the level of purity p in the initial state on correlated coherence and quantum discord for both considered states ρ_1^t and ρ_2^t . When $p = 0$, the system presents zero coherence and zero discord since the initial state (18) reduces to $\rho^{t=0} = \rho_1^{t=0} = \rho_2^{t=0} = \frac{1}{4}I_4$ which is an incoherent separable state. As it is shown in Fig. 5a, b, the evolved density matrix corresponding to $p = 0$ does not contain discord-type

Fig. 3 Time-evolution of coherence 3a and quantum correlations 3b. Case 1 ($\rho^t \equiv \rho_1^t$): versus Γ_z . Case 2 ($\rho^t \equiv \rho_2^t$): versus J

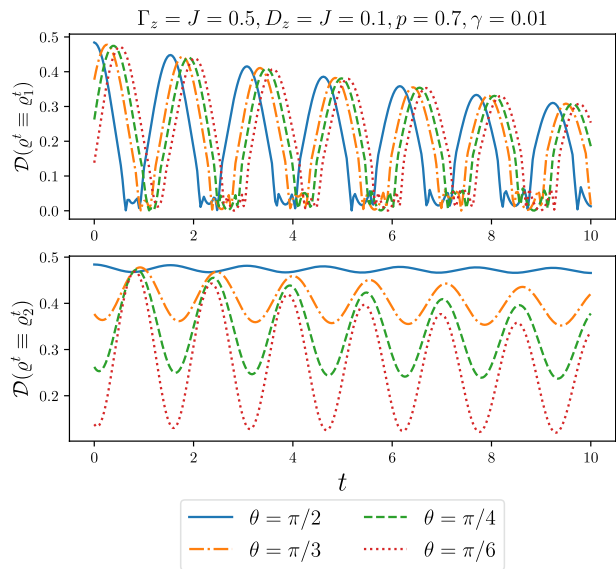


correlations ($\mathcal{D}(\rho_1^t) = \mathcal{D}(\rho_2^t) = 0$) nor correlated coherence ($C_{cc}(\rho_1^t) = C_{cc}(\rho_2^t) = 0$). Raising the purity level, p , improves quantum correlations and coherence within the system, whereas it does not affect the frequency of their oscillations. Both quantifiers, given both cases $\rho^{t=0} = \rho_1^{t=0}$ and $\rho^{t=0} = \rho_2^{t=0}$, display damped oscillations. Nevertheless, we recognize in the first case the collapse and revival phenomenon, which is not manifested when $\rho^{t=0} = \rho_2^{t=0}$. As mentioned earlier, the initial amounts of quantum discord and correlated

Fig. 4 Time-evolution of coherence **(a)** and quantum correlations **(b)**. Case 1 ($\rho' \equiv \rho'_1$) and case 2 ($\rho' \equiv \rho'_2$), versus the Bloch angle θ



(a)



(b)

coherence in the system are those of the initial state given, so it is only natural that they are exclusively dependent on the purity level p and the angle θ . In all figures, it can be seen that the values of quantum coherence and correlations for both cases are the same before the system starts to evolve (at $t = 0$). This is because both Bell-like states have the same superposition and the same amount of entanglement. Furthermore, correlated coherence is

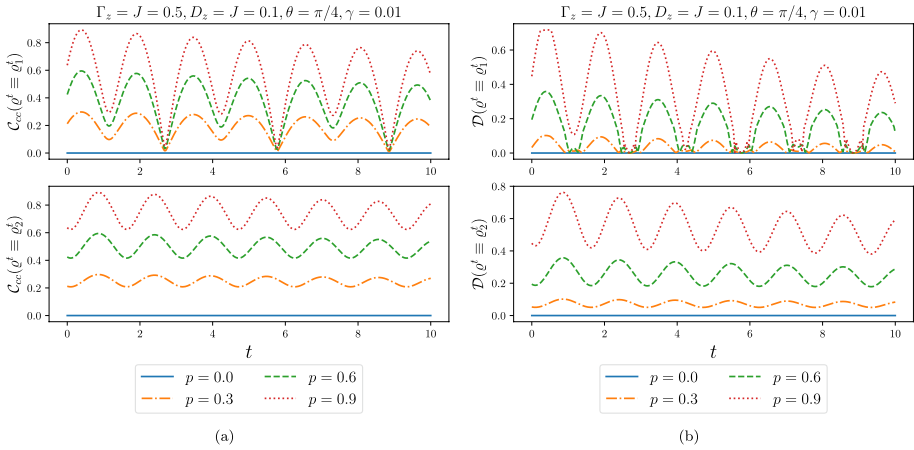


Fig. 5 Time-evolution of coherence 5a and quantum correlations 5b. Case 1 ($\rho^t \equiv \rho_1^t$) and case 2 ($\rho^t \equiv \rho_2^t$), versus the level of purity p

always more significant than the nonclassical correlations measured by QD for both initial states.

5 Conclusion

By utilizing correlated coherence and quantum discord, the dynamics of correlated coherence and quantum discord versus intrinsic decoherence rate are investigated in the two-spin XXZ model under the interplay of two different types of interactions. We found that correlated coherence and quantum discord dynamics depend on all system parameters except the anisotropy coupling J_z , which has no effects. The two measures go up and down in a pattern that gets smaller and quieter as time passes. In particular, we find that the initial state affects the system’s dynamics significantly because it allows it to avoid specific interactions. We also found that the maximum value of the steady state gets smaller by increasing B, Γ_z , and D_z , but increasing J makes the steady state bigger. We show that it is possible to have more robust quantum resources by engineering an appropriate initial state for the system. Moreover, we found that the exchange of information between the system and the magnetic field causes quantum discord to have irregular oscillations for the case $\rho^t \equiv \rho_1^t$. We note that the only part contributing to the correlated coherence dynamic is total coherence because local coherence is always zero, meaning that the reduced density matrices of the subsystems are incoherent states. The results of this work give a more in-depth understanding of the influence of specific interactions and initial state and their consequences on the coherence and discord dynamics of the considered quantum system.

Acknowledgements Z. D expresses special thanks to the Abdus Salam International Centre for Theoretical Physics (ICTP) for the hospitality and for providing access to their research facilities during his visit, which helped accomplish some of this work. M. O acknowledges the financial support received from the National Center for Scientific and Technical Research (CNRST) under the Program of Excellence Grants for Research.

Author Contributions ZD developed the theoretical formalism, performed the analytic calculations and performed the numerical simulations. MO contributed to writing the initial draft and discussion of the manuscript. MM supervised the project. All authors reviewed the final draft of the manuscript.

Funding This work did not receive any funding.

Data availability statement This work is theoretical and all data is in the manuscript.

Declarations

Conflict of interest The authors declare that there no competing interests.

Ethical approval Not applicable

References

- Adesso, G., Bromley, T.R., Cianciaruso, M.: Measures and applications of quantum correlations. *J. Phys. A: Math. Theor.* **49**(47), 473001 (2016)
- Ali, M., Rau, A., Alber, G.: Erratum: Quantum discord for two-qubit X states [*Phys. Rev. A* **81**, 042105 (2010)]. *Phys. Rev. A* **82**(6), 069902 (2010)
- El Anouz, K., Onyenegecha, C., Opara, A., Salah, A., El Allati, A.: Dynamics of quantum Fisher information and quantum coherence of two interacting atoms under time-fractional analysis. *JOSA B* **39**(4), 979–989 (2022)
- Baba, H., Kaydi, W., Daoud, M., Mansour, M.: Entanglement of formation and quantum discord in multipartite j -spin coherent states. *Int. J. Mod. Phys. B* **34**(26), 2050237 (2020)
- Baumgratz, T., Cramer, M., Plenio, M.B.: Quantifying coherence. *Phys. Rev. Lett.* **113**(14), 140401 (2014)
- Chaouki, E., Dahbi, Z., Mansour, M.: Dynamics of quantum correlations in a quantum dot system with intrinsic decoherence effects. *Int. J. Mod. Phys. B* **36**(22), 2250141 (2022)
- Chen, Q., Zhang, C., Yu, S., Yi, X.X., Oh, C.H.: Quantum discord of two-qubit X states. *Phys. Rev. A* **84**, 042313 (2011)
- Citro, R., Orignac, E.: Effects of anisotropic spin-exchange interactions in spin ladders. *Phys. Rev. B* **65**(13), 134413 (2002)
- Coopmans, L., Kiely, A., De Chiara, G., Campbell, S.: Optimal control in disordered quantum systems. *arXiv preprint arXiv:2201.02029* (2022)
- Cruz, C., Anka, M.F., Reis, M.S., Bachelard, R., Santos, A.C.: Quantum battery based on quantum discord at room temperature. *Quantum Sci. Technol.* **7**(2), 025020 (2022)
- Dahbi, Z., Mansour, M., El Allati, A.: Dynamics of quantum correlations in two 2-level atoms coupled to thermal reservoirs. *Phys. Scr.* **98**(1), 015102 (2023)
- Dahbi, Z., Rahman, A.U., Mansour, M.: Skew information correlations and local quantum fisher information in two gravitational cat states. *Phys. A: Stat. Mech. Appl.* **609**, 128333 (2022)
- Dahbi, Z., Anka, M.F., Mansour, M., Rojas, M., Cruz, C.: Effect of induced transition on the quantum entanglement and coherence in two-coupled double quantum dots system. *arXiv e-prints*, pp. arXiv–2211 (2022)
- Doggen, E.V., Schindler, F., Tikhonov, K.S., Mirlin, A.D., Neupert, T., Polyakov, D.G., Gornyi, I.V.: Many-body localization and delocalization in large quantum chains. *Phys. Rev. B* **98**(17), 174202 (2018)
- Dowling, J.P., Milburn, G.J.: “Quantum technology: the second quantum revolution,” *Philosophical transactions of the royal society of London. Seri. A Math. Phys. Eng. Sci.* **361**(1809), 1655–1674 (2003)
- Einstein, A., Podolsky, B., Rosen, N.: Can quantum-mechanical description of physical reality be considered complete? *Phys. Rev.* **47**(10), 777 (1935)
- Ekert, A.K., Rarity, J.G., Tapster, P.R., Palma, G.M.: Practical quantum cryptography based on two-photon interferometry. *Phys. Rev. Lett.* **69**(9), 1293 (1992)
- Elghaayda, S., Dahbi, Z., Mansour, M.: Local quantum uncertainty and local quantum Fisher information in two-coupled double quantum dots. *Opt. Quant. Electron.* **54**(7), 1–15 (2022)
- Elghaayda, S., Dahbi, Z., Mohamed, A.B., Mansour, M.: Nonlocal quantum correlations in a bipartite quantum system coupled to a bosonic non-Markovian reservoir. *Modern Phys. Lett. A* **37**, 2250175 (2022)
- Essakhi, M., Khedif, Y., Mansour, M., Daoud, M.: Intrinsic decoherence effects on quantum correlations dynamics. *Opt. Quant. Electron.* **54**(2), 1–15 (2022)

- Fanchini, F., Werlang, T., Brasil, C., Arruda, L., Caldeira, A.: Non-Markovian dynamics of quantum discord. *Phys. Rev. A* **81**(5), 052107 (2010)
- Ferreira, M., Rojas, O., Rojas, M.: Thermal entanglement and quantum coherence of a single electron in a double quantum dot with Rashba Interaction. arXiv preprint [arXiv:2203.06301](https://arxiv.org/abs/2203.06301) (2022)
- Filgueiras, C., Rojas, O., Rojas, M.: Thermal entanglement and correlated coherence in two coupled double quantum dots systems. *Ann. Phys.* **532**(8), 2000207 (2020)
- Haddadi, S., Hu, M.-L., Khedif, Y., Dolatkah, H., Pourkarimi, M.R., Daoud, M.: Measurement uncertainty and dense coding in a two-qubit system: Combined effects of bosonic reservoir and dipole-dipole interaction. *Results Phys.* **32**, 105041 (2022)
- Haddadi, S., Pourkarimi, M.R., Akhound, A., Ghominejad, M.: Thermal quantum correlations in a two-dimensional spin star model. *Mod. Phys. Lett. A* **34**(22), 1950175 (2019)
- Hashem, M., Mohamed, A.-B.A., Haddadi, S., Khedif, Y., Pourkarimi, M.R., Daoud, M.: Bell nonlocality, entanglement, and entropic uncertainty in a Heisenberg model under intrinsic decoherence: DM and KSEA interplay effects. *Appl. Phys. B* **128**(4), 1–10 (2022)
- Henderson, L., Vedral, V.: Classical, quantum and total correlations. *J. Phys. A: Math. Gen.* **34**, 6899 (2001)
- Henderson, L., Vedral, V.: Classical, quantum and total correlations. *J. Phys. A: Math. Gen.* **34**(35), 6899 (2001)
- Huang, Y.: Quantum discord for two-qubit X states: analytical formula with very small worst-case error. *Phys. Rev. A* **88**(1), 014302 (2013)
- Huang, Y.: Computing quantum discord is NP-complete. *New J. Phys.* **16**(3), 033027 (2014)
- Kaplan, T.: Single-band hubbard model with spin-orbit coupling. *Zeitschrift für Physik B Condensed Matter* **49**(4), 313–317 (1983)
- Khedif, Y., Haddadi, S., Pourkarimi, M.R., Daoud, M.: Thermal correlations and entropic uncertainty in a two-spin system under DM and KSEA interactions. *Mod. Phys. Lett. A* **36**(29), 2150209 (2021)
- Kim, Y.-H., Kulik, S.P., Shih, Y.: Quantum teleportation of a polarization state with a complete Bell state measurement. *Phys. Rev. Lett.* **86**(7), 1370 (2001)
- Lambert, N., Chen, Y.-N., Cheng, Y.-C., Li, C.-M., Chen, G.-Y., Nori, F.: Quantum biology. *Nat. Phys.* **9**(1), 10–18 (2013)
- Li, B.-M., Hu, M.-L., Fan, H.: Nonlocal advantage of quantum coherence and entanglement of two spins under intrinsic decoherence. *Chin. Phys. B* **30**(7), 070307 (2021)
- Luo, S.: Quantum discord for two-qubit systems. *Phys. Rev. A* **77**(4), 042303 (2008)
- Maleki, Y.: Entanglement and decoherence in two-dimensional coherent state superpositions. *Int. J. Theor. Phys.* **56**(3), 757–770 (2017)
- Malvezzi, A., Karpat, G., Çakmak, B., Fanchini, F., Debarba, T., Vianna, R.: Quantum correlations and coherence in spin-1 Heisenberg chains. *Phys. Rev. B* **93**(18), 184428 (2016)
- Mansour, M., Dahbi, Z.: Entanglement of bipartite partly non-orthogonal-spin coherent states. *Laser Phys.* **30**(8), 085201 (2020)
- Mansour, M., Dahbi, Z.: Quantum secret sharing protocol using maximally entangled multi-qudit states. *Int. J. Theor. Phys.* **59**(12), 3876–3887 (2020)
- Mansour, M., Oulouda, Y., Sbiri, A., Falaki, M.E.: Decay of negativity of randomized multiqubit mixed states. *Laser Phys.* **31**(3), 035201 (2021)
- Melo-Luna, C.A., Susa, C.E., Ducuara, A.F., Barreiro, A., Reina, J.H.: Quantum locality in game strategy. *Sci. Rep.* **7**(1), 1–11 (2017)
- Milburn, G.: Intrinsic decoherence in quantum mechanics. *Phys. Rev. A* **44**(9), 5401 (1991)
- Mofidnakhai, F., Khastehdel Fumani, F., Mahdavi, S., Vahedi, J.: Quantum correlations in anisotropic XY-spin chains in a transverse magnetic field. *Phase Transit.* **91**(12), 1256–1267 (2018)
- Mohamed, A.-B.A., Abdel-Aty, A.-H., Qasymeh, M., Eleuch, H.: Non-local correlation dynamics in two-dimensional graphene. *Sci. Rep.* **12**(1), 1–12 (2022)
- Mohamed, A.-B.A., Eleuch, H.: Quasi-probability information in a coupled two-qubit system interacting non-linearly with a coherent cavity under intrinsic decoherence. *Sci. Rep.* **10**(1), 1–11 (2020)
- Mohamed, A.A., Eleuch, H.: Thermal local fisher information and quantum uncertainty in Heisenberg model. *Phys. Scr.* **97**(9), 095105 (2022)
- Mohamed, A.B.A., Khedr, A.N., Haddadi, S., Rahman, A.U., Tammam, M., Pourkarimi, M.R.: Intrinsic decoherence effects on nonclassical correlations in a symmetric spin-orbit model. *Result Phys.* **39**, 105693 (2022)
- Mohamed, A.-B.A., Rahman, A.U., Eleuch, H.: Measurement uncertainty, purity, and entanglement dynamics of maximally entangled two qubits interacting spatially with isolated cavities: intrinsic decoherence effect. *Entropy* **24**(4), 545 (2022)
- Moriya, T.: Anisotropic superexchange interaction and weak ferromagnetism. *Phys. Rev.* **120**(1), 91 (1960)

- Muthuganesan, R., Chandrasekar, V.: Intrinsic decoherence effects on measurement-induced nonlocality. *Quantum Inf. Process.* **20**(1), 1–15 (2021)
- Narasimhachar, V., Gour, G.: Low-temperature thermodynamics with quantum coherence. *Nat. Commun.* **6**(1), 1–6 (2015)
- Naveena, P., Muthuganesan, R., Chandrasekar, V.: Effects of intrinsic decoherence on quantum correlations in a two superconducting charge qubit system. *Physica A* **592**, 126852 (2022)
- Nielsen, M.A., Chuang, I.: *Quantum computation and quantum information* (2002)
- Obada, A.-S., Hessien, H.A., Mohamed, A., Hashem, M.: Influence of the phase damping for two-qubits system in the dispersive reservoir. *Quantum Inf. Process.* **12**(5), 1947–1956 (2013)
- Ollivier, H., Zurek, W.H.: Quantum discord: a measure of the quantumness of correlations. *Phys. Rev. Lett.* **88**(1), 017901 (2001)
- Oumennana, M., Dahbi, Z., Mansour, M., Khedif, Y.: Geometric measures of quantum correlations in a two-qubit heisenberg XXZ model under multiple interactions. *Effects. J. Russ. Laser Res.* **43**(5), 533–545 (2022)
- Oumennana, M., Rahman, A.U., Mansour, M.: Quantum coherence versus non-classical correlations in XXZ spin-chain under Dzyaloshinsky–Moriya (DM) and KSEA interactions. *Appl. Phys. B* **128**(9), 1–13 (2022)
- Pan, F., Qiu, L., Liu, Z.: The complementarity relations of quantum coherence in quantum information processing. *Sci. Rep.* **7**(1), 1–8 (2017)
- Pires, D.P., Silva, I.A., deAzevedo, E.R., Soares-Pinto, D.O., Filgueiras, J.G.: Coherence orders, decoherence, and quantum metrology. *Phys. Rev. A* **98**(3), 032101 (2018)
- Ritz, T.: Quantum effects in biology: bird navigation. *Procedia Chem.* **3**(1), 262–275 (2011)
- Schlosshauer, M.: Decoherence, the measurement problem, and interpretations of quantum mechanics. *Rev. Mod. Phys.* **76**(4), 1267 (2005)
- Schlosshauer, M.: Quantum decoherence. *Phys. Rep.* **831**, 1–57 (2019)
- Scholes, G.D.: Coherence in photosynthesis. *Nat. Phys.* **7**(6), 448–449 (2011)
- Shekhtman, L., Entin-Wohlman, O., Aharony, A.: Moriya's anisotropic superexchange interaction, frustration, d dzyaloshinsky's weak ferromagnetism. *Phys. Rev. Lett.* **69**(5), 836 (1992)
- Tan, K.C., Kwon, H., Park, C.-Y., Jeong, H.: Unified view of quantum correlations and quantum coherence. *Phys. Rev. A* **94**(2), 022329 (2016)
- Wang, C.-Z., Li, C.-X., Nie, L.-Y., Li, J.-F.: Classical correlation and quantum discord mediated by cavity in two coupled qubits. *J. Phys. B: At. Mol. Opt. Phys.* **44**(1), 015503 (2010)
- Werner, R.F.: Quantum states with Einstein–Podolsky–Rosen correlations admitting a hidden-variable model. *Phys. Rev. A* **40**(8), 4277 (1989)
- Wu, Y.-L., Deng, D.-L., Li, X., Sarma, S.D.: Intrinsic decoherence in isolated quantum systems. *Phys. Rev. B* **95**(1), 014202 (2017)
- Xie, Y.-X., Liu, X.-Y.: Enhancing steered coherence in the Heisenberg model using Dzyaloshinsky–Moriya and Kaplan–Shekhtman–Entin–Wohlman–Aharony interactions. *Laser Phys. Lett.* **19**(2), 025204 (2022)
- Yin, S., Liu, S., Song, J., Luan, H.: Markovian and non-Markovian dynamics of quantum coherence in the extended X X chain. *Phys. Rev. A* **106**(3), 032220 (2022)
- Yuan, X., Zhou, H., Cao, Z., Ma, X.: Intrinsic randomness as a measure of quantum coherence. *Phys. Rev. A* **92**(2), 022124 (2015)

Publisher's Note Springer Nature remains neutral with regard to jurisdictional claims in published maps and institutional affiliations.

Springer Nature or its licensor (e.g. a society or other partner) holds exclusive rights to this article under a publishing agreement with the author(s) or other rightsholder(s); author self-archiving of the accepted manuscript version of this article is solely governed by the terms of such publishing agreement and applicable law.